Developing Real-Time System Identification for UAVs

Pierre-Daniel Jameson *, Alastair Cooke †

School of Engineering
Department of Aircraft Enginering
Dynamics, Simulation, and Control Group
Cranfield University, Bedfordshire
United Kingdom
Email: p.d.jameson@cranfield.ac.uk*, a.k.cooke@cranfield.ac.uk†

Abstract—This work is based on adapting suitable techniques in real-time aircraft system identification for the use in rigid body dynamic modelling of Unmanned Aerial Vehicles (UAVs). In general due to their reduced size UAVs lend themselves well to the recovery of flight data in full scale atmospheric trials. Timely recovery of the true model parameters is necessary to minimise flight tests for rapid prototype development. Using the Cranfield University Jetstream-31 Flying Laboratory (G-NFLA) as a test bed an investigation into suitable parameter update methods applicable for UAV purposes is being performed; and builds on previous work which considered the constraints pertinent to small UAVs, such as the absence of air flow vanes.This paper outlines an approach to achieve post-manoeuvre parameter estimation by applying the equation-error method in the frequency domain, and an example using flight data for the Jestream-31 flying laboratory is presented.

I. INTRODUCTION

A. Background

With the evolution of aircraft design and manufacture, flight testing still remains an integral aspect of the process; however, commercial demands require that a flight campaign achieve its goals in the minimal time possible. Advances in simulation and wind-tunnel modelling enable us to better predict aircraft dynamics which are necessary for the development of flight control laws, and provide the starting point for full-scale trials. Numerous examples of aircraft system identification (SysID) to determine suitable dynamic models for manned aircraft are widely reported [1], [2]. Despite the rapid development of UAV platforms widespread application of this technique has yet to occur in the unmanned field.

Real-time SysID was primarily driven by the need to monitor highly unstable aircraft behaviour in non-linear flight regimes, while expanding the operational flight envelope [3]. Recent development has focused on creating self-healing control systems, such as adaptive re-configurable control laws to provide robustness against airframe damage or control surface failures [4], [5]. In the case of UAVs real-time identification, would facilitate rapid prototyping especially in low-cost projects with their constrained development time. Development of SysID for a small UAV scenario could lead to flight trials focused towards dynamic model validation, with the prior verification step done using the simulation environment.

Therefore, current research in the department is primarily concerned with developing post-manoeuver estimation of the aerodynamic derivatives, and builds on the work undertaken by Carnduff [6] which outlined SysID methods for UAVs. The ability to check the estimated derivatives while the aircraft is flying would enable detection of poor data readings due to deficient excitation manoeuvres or atmospheric turbulence. Subsequently, appropriate action could then be taken while all the equipment and personnel are in place.

B. Aircraft system identification

A brief explanation of key points relating to the process of aircraft SysID will now follow, an in-depth explanation can be found in [7]. The conventional SysID method can be seen in figure 1, the process depends on the *a priori* knowledge about the aircraft and is then followed by five distinct steps: experiment design, Data Compatibility Check (DCC), model structure determination, parameter estimation and model validation.
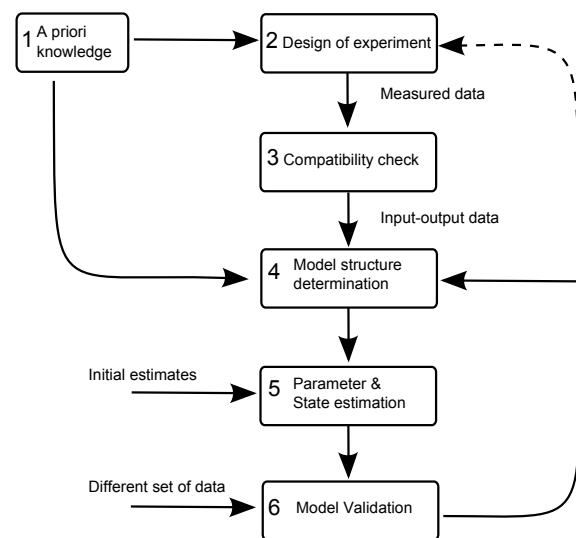

Fig. 1. An overview of the SysID process, [8].

The experiment design relates to the type of input used to perturb the aircraft from an initial state of balanced forces

Fig. 2. The Cranfield Jetstream-31 flying laboratory

and moments defined as *trim*, chosen to be a steady level flight condition for this study. The DCC step processes the data for kinematic consistency between the inertial and air data, thus allowing sensor errors or data drop-outs to be dealt with. In certain cases the model structure for the aircraft is then determined from the data, the model is then populated with the estimated model parameters and states. Finally, the representative model is validated by using a separate data set not previously used during the modelling process. Should a validation fail, alternative model structures or estimation techniques should be trialled before making the expensive decison to use a different excitation input (dotted line in figure 1). From *a priori* knowledge of the aircraft: the data was known to be compatible therefore the DCC step was neglected, and reduced order models were postulated eneabling the SysID process to proceeded directly to the Parameter Estimation (PE) step.

C. Jetstream Aircraft

G-NFLA shown in figure 2 operates as the United Kingdom's National Flying Laboratory Aircraft and is primarily used to demonstrate flight dynamics principles to undergraduate students. As a result the types of excitation inputs used are limited to impulses and doublets. The aircraft is instrumented with an Inertial Reference System (IRS), GPS, and air data probes. Displays in-front of every seat (similar to an in-flight entertainment display) are driven by an on-board computer which transforms the measured data into strip-charts and guages depending on the topic being covered. It is anticipated that this computer will be used to run the parameter estimation algorithms; therefore an emphasis has been placed on incurring minimal additional computational burden. Current practice is to retrieve the recorded flight data from the computer hard drive for post-flight analysis using a USB key.

D. Motivation

The aim of the current work is to develop a flexible tool box for post-manoeuver parameter estimation for UAVs. Using G-NFLA as a flying test-bed, suitable algorithms have been tested with postulated models for the reduced order SPPO, and Dutch Roll modes. As flight test data is primarily available on an opportunistic basis, the ability to reduce processing time would maximise such opportunities.

II. METHOD

A. Models

From the *a priori* knowledge about the aircraft, the standard rigid body equations of motion can be used to formulate a model which accurately describes the aircraft dynamics. The assumption when using such models is that the longitudinal and lateral dynamics are suitably distinct in order to be decoupled. The following body axes models are taken from [9], where the SPPO model is:

$$\begin{bmatrix} \dot{\boldsymbol{W}} \\ \dot{\boldsymbol{q}} \end{bmatrix} = \begin{bmatrix} Z_w & Z_q \\ M_w & M_q \end{bmatrix} \begin{bmatrix} \boldsymbol{W} \\ \boldsymbol{q} \end{bmatrix} + \begin{bmatrix} Z_\eta \\ M_\eta \end{bmatrix} [\boldsymbol{\eta}] \qquad (1)$$

and the Dutch Roll model is:

$$\begin{bmatrix} \dot{\boldsymbol{V}} \\ \dot{\boldsymbol{r}} \end{bmatrix} = \begin{bmatrix} Y_v & Y_r \\ N_v & N_r \end{bmatrix} \begin{bmatrix} \boldsymbol{V} \\ \boldsymbol{r} \end{bmatrix} + \begin{bmatrix} Y_\zeta \\ N_\zeta \end{bmatrix} [\boldsymbol{\zeta}] \qquad (2)$$

Here it must be noted that the above stability and control derivatives are in concise form, and therefore require manipulation in order to relate them to the respective non-dimensional values (see appendix of [9]).

B. Body Translational Rates

Typically, large aircraft can be readily equipped to measure air data using α- or β-vanes; these measurements enable the body translational rates: u_b, v_b and w_b to be determined and form part of the dependent variables shown in equations 1 and 2. In smaller UAVs access to such air data measurements can prove unfeasible. In the absence of these vanes, measurements from an IRS can be used to calculate the translational rates (see [10], [11]). These rates can be determined using 'track-fixed' accelerations; neglecting turbulence the IRS has more reliable sensors with respect to the analog vane type instruments.

C. Frequency Domain Transformation

With reference to Klein [12] and more recently Morelli [13] the Equation-Error method in the frequency domain can be formulated. Analysis in the frequency domain using the finite Fourier Transform method is better suited to the linear model identification being considered for two key points. Firstly, when the Fourier transform is applied the bias and drift in the measured data is removed. Secondly, using *a priori* knowledge of the expected frequency range the data to be analysed can be easily reduced. Further to the above benefits, differentiation and convolution in the frequency domain simplifies to multiplication by $j\omega$, allowing terms such as $\dot{p}$, $\dot{q}$, $\dot{r}$ and $\dot{u}_b$, $\dot{v}_b$, $\dot{w}_b$ to be calculated. Considering the aircraft model in state space form:

$$\dot{x}(t) = \mathbf{A}x(t) + \mathbf{B}u(t), \ x(0) = 0 \qquad (3)$$
$$y(t) = \mathbf{C}x(t) + \mathbf{D}u(t) \qquad (4)$$
$$z(t) = y(t) + \nu(t) \qquad (5)$$

where *x(t)*, *u(t)*, and *y(t)* are the state, input and output vectors, *z(t)* is the measurement equation with error $\nu(t)$. Unknowns within **A**, **B**, **C**, and **D** are assigned to the unknown parameter matrix, $\boldsymbol{\theta}$.

Equation 6 is the Fourier transform associated with *x(t)* for the finite time interval [0, *T*], a simple Euler approximation can be implemented resulting in equation 7.

$$\tilde{x}(\omega) = \int_0^T x(t)e^{-j\omega}dt \qquad (6)$$

$$\tilde{x}(\omega) \approx \Delta t \sum_{i=0}^{N-1} x(i)e^{-j\omega\Delta t} \qquad (7)$$

where the complex number $j = \sqrt{-1}$, $\omega =$ is the angular frequency, i is the discrete time index, Δt is the sampling interval, and $N + 1$ is the total number of data points. The summation on the right in equation 7 is known as the Discrete Fourier Transform (DFT), $\tilde{X}(\omega)$:

$$\tilde{X}(\omega) = \sum_{i=0}^{N-1} x(i)e^{-j\omega\Delta t} \qquad (8)$$

thus equation 7 can be written as:

$$\tilde{x}(\omega) = \tilde{X}(\omega)\Delta t \qquad (9)$$

As equation 9 is effectively a first order Euler approximation [14] of equation 6 corrections such as those outlined by Morelli [15] can be made to account for the inaccuracies. However, by selecting a sampling rate much greater than the frequencies of interest (a small Δt) these corrections can be suitably neglected. Therefore, the Fourier transform for the linear model given in equations 3, and 4 can be expressed:

$$j\boldsymbol{\omega}\tilde{\boldsymbol{x}}(\boldsymbol{\omega}) = \mathbf{A}\tilde{\boldsymbol{x}}(\boldsymbol{\omega}) + \mathbf{B}\tilde{\boldsymbol{u}}(\boldsymbol{\omega}) \qquad (10)$$

$$\tilde{\boldsymbol{y}}(\boldsymbol{\omega}) = \mathbf{C}\tilde{\boldsymbol{x}}(\boldsymbol{\omega}) + \mathbf{D}\tilde{\boldsymbol{u}}(\boldsymbol{\omega}) \qquad (11)$$

Provided that the state, outputs and inputs variables are measured the individual state or output (equation 10 and 11 respectively) can be formulated using the equation error method to estimate the stability and control derivatives in $\boldsymbol{A}, \boldsymbol{B}, \boldsymbol{C}$, and $\boldsymbol{D}$.

D. Equation Error

It can be seen that the least squares cost function in the frequency domain for the kth state vector of equation 10 is:

$$J_k = \frac{1}{2}\sum_{n-1}^{m}|j\omega_n\tilde{x}_k(n) - \boldsymbol{A}_k\tilde{\boldsymbol{x}}(n) - \boldsymbol{B}_k\tilde{\boldsymbol{u}}(n)|^2 \qquad (12)$$

where $\tilde{\boldsymbol{x}}(n)$ and $\tilde{\boldsymbol{u}}(n)$ denote the Fourier transform of the state and control vectors for frequency ω_n. Equation 11 can also be formulated as above for the relavent output equations. As rigid body aircraft dynamics typically lie below 2Hz, the m frequencies of interest in the summation of equation 12 were performed at 0.04Hz intervals from 0.01 - 2Hz, [16]. By neglecting the zero frequency which corresponds to the *trim* and measurement biases, the respective initial conditions no longer need to be estimated for the cost function. Now grouping the unknowns from $\boldsymbol{A}_k$ and $\boldsymbol{B}_k$ into $\boldsymbol{\theta}$, the standard least squares formulation for the complex data is:

$$\boldsymbol{Y} = \boldsymbol{X}\boldsymbol{\theta} + \boldsymbol{\epsilon} \qquad (13)$$

expanding the vectors:

$$\boldsymbol{Y}^T \equiv [j\omega_1\tilde{x}_k(1), j\omega_2\tilde{x}_k(2), \ldots, j\omega_m\tilde{x}_k(m)] \qquad (14)$$

$$\boldsymbol{X}^T \equiv [\tilde{\boldsymbol{x}}(1)\ \tilde{\boldsymbol{u}}(1), \tilde{\boldsymbol{x}}(2)\ \tilde{\boldsymbol{u}}(2), \ldots, \tilde{\boldsymbol{x}}(m)\ \tilde{\boldsymbol{u}}(m)] \qquad (15)$$

and $\boldsymbol{\epsilon}$ is the complex equation error in the frequency domain; the cost function to be minimised is identical to that in equation 12 where "†" denotes the complex conjugate:

$$J = \frac{1}{2}(\boldsymbol{Y} - \boldsymbol{X})^\dagger(\boldsymbol{Y} - \boldsymbol{X}) \qquad (16)$$

$$\hat{\boldsymbol{\theta}} = \left[Re(\boldsymbol{X}^\dagger\boldsymbol{X})\right]^{-1} Re(\boldsymbol{X}^\dagger\boldsymbol{Y}) \qquad (17)$$

and the estimated parameter covariance matrix is:

$$cov(\hat{\boldsymbol{\theta}}) \equiv E\left\{(\hat{\boldsymbol{\theta}} - \boldsymbol{\theta})(\hat{\boldsymbol{\theta}} - \boldsymbol{\theta})^T\right\} = \sigma^2 \left[Re(\boldsymbol{X}^\dagger\boldsymbol{X})\right]^{-1} \qquad (18)$$

the equation error variance, $\boldsymbol{\sigma}^2$ is estimated from the residuals:

$$\boldsymbol{\sigma}^2 = \frac{1}{(m - n_p)} \left[(\boldsymbol{Y} - \boldsymbol{X}\hat{\boldsymbol{\theta}})^\dagger(\boldsymbol{Y} - \boldsymbol{X}\hat{\boldsymbol{\theta}})\right] \qquad (19)$$

where n_p is the number of parameter elements in $\boldsymbol{\theta}$, and the parameter standard errors can be calculated by using equation 19 and then square rooting the diagonal elements of matrix $cov(\hat{\boldsymbol{\theta}})$ in equation 18.

E. Real-time parameter estimation in frequency domain

Current real-time methods include: Recursive Least Squares (RLS), Extended Kalman Filter (EKF), and batch estimation methods (seen as sequential least squares) [17]. Identification in the cases of fault-detection and reconfigurable control requires immediate results (use RLS and EKF). In comparison for dynamic modelling, a near real-time capability is acceptable (use batch estimation method). Batch methods use strips of data at defined time intervals to approximate the time variation in the parameters and enable principally off-line methods such as the least squares technique to be used in a real-time setting. In order to gain the benefits of working in the frequency domain, a recursive finite Fourier transform (RFT) can be coupled with the sequential least squares.

With reference to the discrete Fourier transform (equation 8) the RFT for a specific frequency of interest $\boldsymbol{\omega}$, at sample time $i\Delta t$ can be related to the result at sample time $(i - 1)\Delta t$ as follows:

$$X_i(\boldsymbol{\omega}) = X_{i-1}(\boldsymbol{\omega}) + x_i e^{-j\boldsymbol{\omega}i\Delta t} \qquad (20)$$

with

$$e^{-j\boldsymbol{\omega}\Delta t} = e^{-j\boldsymbol{\omega}t}e^{-j\boldsymbol{\omega}(i-1)\Delta t} \qquad (21)$$

Note that $e^{-j\boldsymbol{\omega}\Delta t}$ is constant for a given frequency ω and sampling interval of Δt. Therefore, equations 20 and 21 enable the data to be transformed for a given frequency with the use of one addition and two multiplications respectively. The time-domain data can be discarded as the RFT behaves as a memory, as the recursion proceeds results for each new sample are added to the overall information held in the constant $e^{-j\boldsymbol{\omega}\Delta t}$ term.

In order to improve the response of the PE to the most recent conditions a selective amnesia, λ, can be applied to the RFT

as in equation 22 to remove past data. The effect of varying λ from 0.95 - 1 can be seen as a type of windowing on the data, this is illustrated in figure 3, when $\lambda = 1$, this results in the case of the general RFT where each data point is given equal weighting.

$$X_i(\boldsymbol{\omega}) = \lambda X_{i-1}(\boldsymbol{\omega}) + x_i e^{-j\boldsymbol{\omega} i \Delta t} \qquad (22)$$
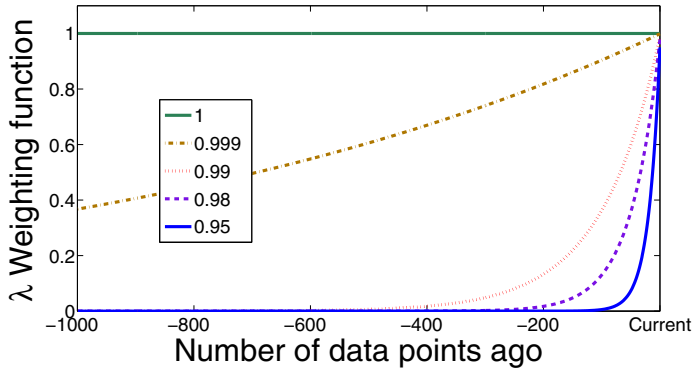
Fig. 3.   Effective window of forgetting factor

For the implementation, data is recorded at 50 Hz and saved in csv format onboard the aircraft. Using Matlab the relevant state measurements for the desired mode are selected and then passed through the RFT of equations 22 and 21 at 1Hz. Subsequently the least-squares estimation is performed at 25Hz using equations 17 - 19. In order to prevent ill-conditioning when implementing equation 17 the first estimation uses 2 seconds of data to allow sufficient information to be gathered.

III. ANALYSIS

The flight trials were conducted at: 6045ft and 170kt (1843m, 87.5m/s) with a center of gravity at 30 % of the Mean Aerodynamic Chord. Two recordings were used, the first set for parameter estimation and the second set as a means of validation. Using *a priori* knowledge of the aircraft empirical estimates[1] of the concise derivatives were calculated for use as reference values. Tests were conducted with the forgetting factor varied from 0.95 - 1, the full results for $\lambda = 1$ and an indicative set of results for $\lambda = 0.98$ are presented below.

A. Longitudinal

Trace plots for the reduced order longitudinal dynamics are shown in Figures 4 and 5, where the empirical estimates are plotted alongside the varying parameter estimates. The longitudinal dynamics were excited by closely coupling two elevator (η) impulses in a positive and negative direction, these are shown in the bottom subplot of each figure. The empirical (Emp) and final estimated (Est) values are listed in table I respectively; the Est values correspond to the finally estimated value at the end of each parameter trace plot and are indicated by a dot. The estimation results for the moment derivatives when a forgetting factor is used are presented in figure 6. Finally, figure 10 shows the prediction response of both sets of data from table I for the pitch rate response for the validation data set at the same flight condition.

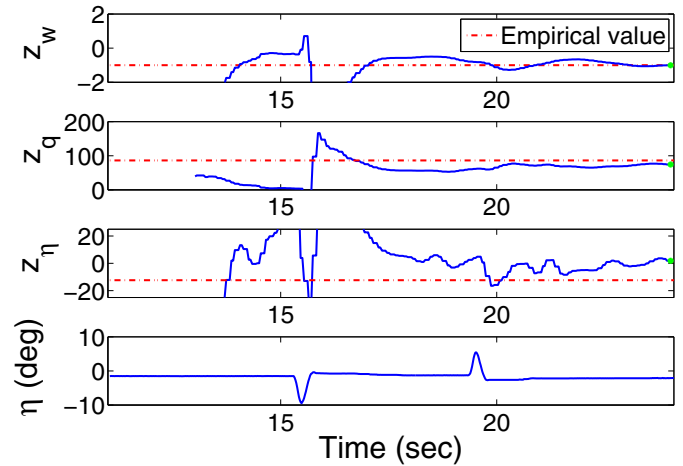[1]Using ESDU, a statistically significant data set and engineering judgment.
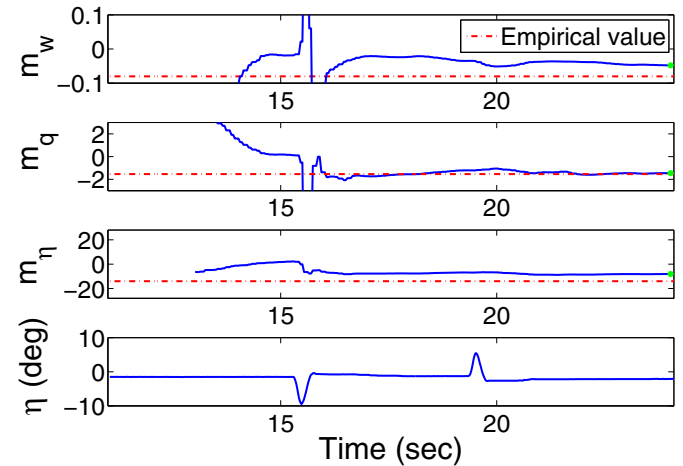

Fig. 4.   SPPO: force derivatives
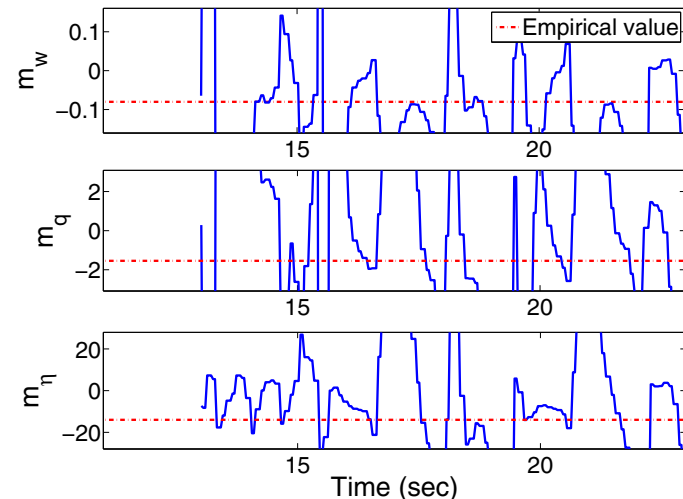

Fig. 5.   SPPO: moment derivatives

Fig. 6.   SPPO: moment derivatives with $\lambda = 0.98$

B. Lateral

The lateral dynamic results are presented in a similar manner as above. In order to excite the lateral dynamics the yaw-damper needs to be disabled, then the pilot drives the mode by applying rudder (ζ) doublets on the pedals as shown in the final subplot of figures 7 and 8.
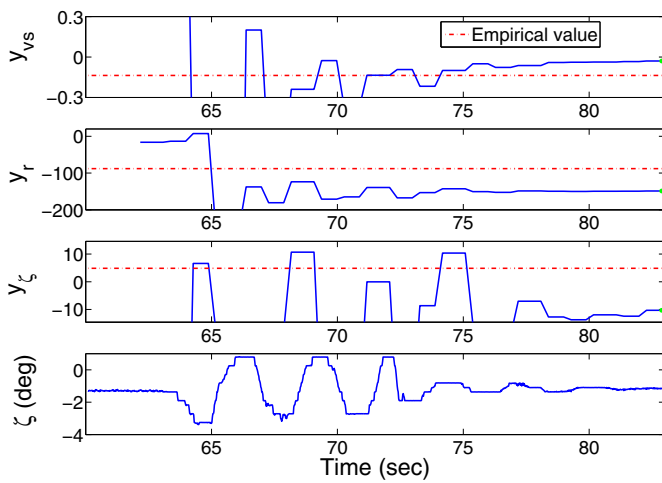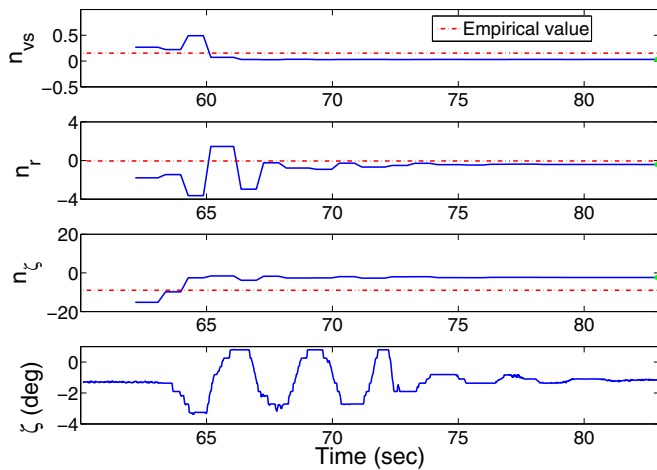
Fig. 7.   DR: force derivatives
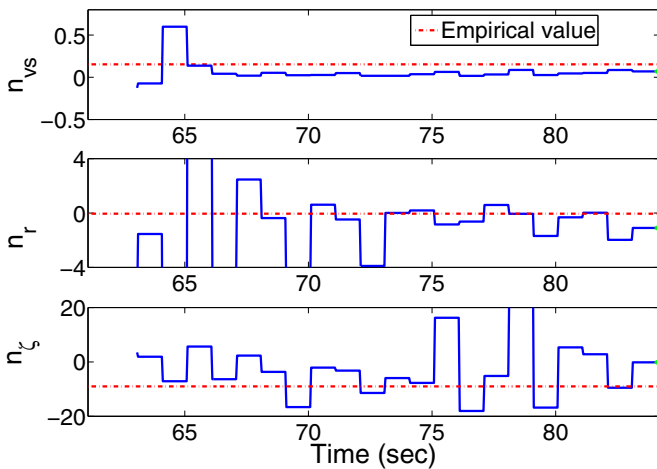

Fig. 8.   DR: moment derivatives

Fig. 9.   DR: moment derivatives with $\lambda = 0.98$

IV. DISCUSSION

Both sets of longitudinal derivatives established constant estimate values by the end of the 25 second data segment. In the case of the force derivatives (figure 4) all three parameters showed an improvement after the initial elevator deflection,
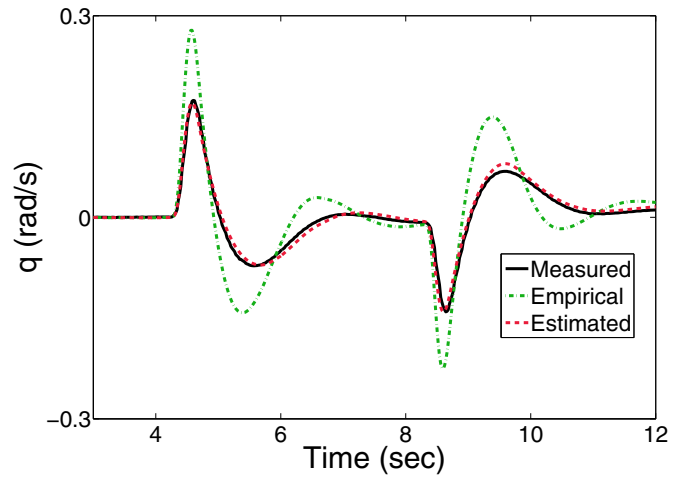

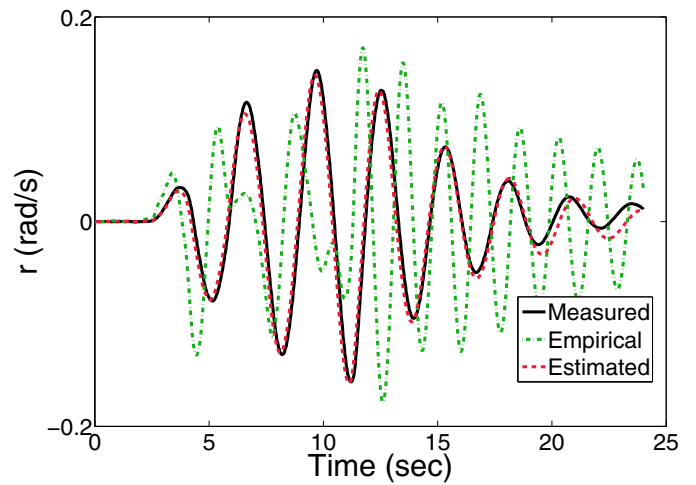Fig. 10.   SPPO: pitch rate validation plot

Fig. 11.   DR: yaw rate validation plot

and a small variability following the second deflection. Following the first input the moment derivatives (figure 5) were close to their steady state values with little variation following the second deflection. By contrast, the derivative estimates using the forgetting factor (figure 6), $\lambda = 0.98$ showed no signs of convergence.

The pitch rate validation plot figure 10 demonstrates that the basic longitudinal dynamics have been captured with the reduced order model, and that the empirical estimates produce an under damped response as could be expected due to the informed approximations used. Referring to table I the majority of the empirical and estimated derivatives compare well. The exception is z_η which has an incorrect sign and a reduced magnitude, however this is also highlighted as having the largest standard error of ± 19.599. Nevertheless, it is important to note that the pitch damping term, m_q (which is a key term for the SPPO mode) closely matches the empirical estimate and has a low standard error, ± 0.554.

For the lateral case the force derivatives in figure 7 displayed a gradual improvement as the excitation manoeuvre progressed. In comparison the moment derivatives converged more rapidly to their respective final values (figure 8). Again

TABLE I
SPPO DERIVATIVES AND STANDARD ERRORS

$\hat{\theta}$	Emp	Est	s
z_w	-1.002	-1.005	0.263
z_q	86.170	74.362	13.125
z_η	-12.377	1.868	19.599
m_w	-0.080	-0.048	0.011
m_q	-1.547	-1.459	0.554
m_η	-14.002	-8.078	0.826

TABLE II
DR DERIVATIVES AND STANDARD ERRORS

$\hat{\theta}$	Emp	Est	s
y_v	-0.137	-0.029	0.051
y_r	-88.004	-148.73	4.829
y_ζ	4.865	-10.308	18.140
n_v	0.153	0.031	0.001
n_r	-0.049	-0.415	0.057
n_ζ	-8.980	-2.389	0.213

for the forgetting factor case, the moment derivatives are seen in figure 9 to exhibit a greater variation. For the validation data set the RFT estimated parameters produced a satisfactory yaw rate prediction in figure 11, with the empirical estimates resulting in an undamped response. In addition, a slightly under damped response can also be seen for the estimated derivatives after 20 seconds, this can possibly be attributed to unmodeled roll effects as the reduced order DR model is predominantly associated with yaw, but by definition DR is a coupled yaw-roll mode.

Comparing the DR derivatives in table II the majority of derivatives do not agree. Considering the two derivatives with the greatest standard errors (s), firstly, the estimated side force due to yaw rate derivative, y_r is ≈ 1.7 times greater than the empirical value. Secondly, the estimated side force due to rudder, y_ζ is of a different sign and order of magnitude in comparison to the empirical value. However, referring to the validation plot the DR mode dynamics would seem to have been captured, and therefore further investigation needs to be undertaken to explain the discrepancies that has been found.

Having analysed results for both the SPPO and DR modes the combined least squares in frequency domain RFT method is a promising solution for the online estimation problem. In the present work incorporating a forgetting factor with the RFT was found to be unsuitable particularly with the limited aircraft excitation manoeuvers available, as the removal of information content proved to be too sensitive. Finally, the ability to restrict the frequency range provides several benefits, firstly it significantly reduces the number of computations for the RFT and secondly, it acts as a filter to reduce the effects of the higher aero-elastic frequencies present (associated with the flexible airframe).

V. CONCLUSION AND FUTURE WORK

A suitable methodology to address on-line estimation for a small UAV in the frequency domain has been outlined, in addition the results of trials using the Cranfield Jetstream-31 have been presented. Areas for further development lie in automatically stopping the batch estimation once the parameter estimates have converged to within a specified accuracy.

Furthermore, there exists the opportunity to enhance the way in which the flight data results are recorded, as the UAV flight envelope is opened. Results for runs in repeat conditions can be incorporated to the data set by taking advantage of the constant $e^{-j\omega\delta t}$ in the RFT and therefore continuing the recursion.

REFERENCES

[1] P. G. Hamel and R. V. Jategaonkar, "Evolution of flight vehicle system identification," *Journal of Aircraft*, vol. 33 (1), pp. 9–28, January - February 1996.

[2] K. W. Iliff, "Parameter estimation for flight vehicles," *Journal of Guidance, Control, and Dynamics*, vol. 12 (5), pp. 609–622, September - October 1989.

[3] K. Basappa and R. Jategaonkar, "Evaluation of recursive methods for aircraft parameter estimation," in *AIAA Atmospheric Flight Mechanics Conference and Exhibit*. Providence, Rhode Island: AIAA-2004-5063, 16th-19th August 2004.

[4] D. G. Ward, J. Monaco, and M. Bodson, "Development and flight testing of a parameter identification algorithm for reconfigurable control," *Journal of Guidance, Control and Dynamics*, vol. 21 (6), pp. 948–956, November - December 1998.

[5] G. Chowdhary, W. M. DeBusk, and E. N. Johnson, "Real-time system identification of a small multi-engine aircraft with structural damage," in *AIAA Infotec@Aerospace*. Atlanta, Georgia: AIAA-2010-3472, 20th-22nd April 2010.

[6] S. D. Carnduff, "System identification of Unmanned Aerial Vehicles," PhD Thesis, Cranfield University, Cranfield, Bedfordshire, 2008.

[7] V. Klein, "Estimation of aircraft aerodynamic parameters from flight data," *Progress in Aerospace Sciences*, vol. 26 (1), pp. 1–77, 1989.

[8] ——, "A review of system identification methods applied to aircraft," The George Washington University, Tech. Rep. Joint Institute for Acoustics and Flight Sciences Report: N83 33901, 1983.

[9] M. V. Cook, *"Flight Dynamic Principles : A linear systems approach to aircraft stability and control"*. Amsterdam: Elsevier, 2007.

[10] P.-D. Jameson and A. Cooke, "Developing system identification for UAVs," in *25th Bristol International UAV Systems Conference*, Bristol, United Kingdom, 12th - 14th April 2010.

[11] E. A. Morelli, "Real-time aerodynamic parameteric estimation without air flow angle measurements," in *AIAA Guidance, Navigation, and Control Conference and Exhibit*. Toronto, Ontario: AIAA-2010-7951, 2nd-5th August 2010.

[12] V. Klein, "Aircraft parameter estimation in frequency domain," in *AIAA Atmospheric Flight Mechanics Conference and Exhibit*. Palo Alto, California: AIAA-1978-1344, 7th - 9th August 1978.

[13] E. A. Morelli, "Real-time parameter estimation in the frequency domain," in *AIAA Guidance, Navigation and Control Conference and Exhibit*. Portland, Oregon: AIAA-99-4043, 9th-11th August 1999.

[14] R. Jategaonkar, *"Flight Vehicle System Identification: A Time Domain Methodology"*. Reston, Virginia: AIAA, 2006.

[15] E. A. Morelli and V. Klein, "Accuracy of aerodynamic model parameters estimated from flight test data," *Journal of Guidance, Control, and Dynamics*, vol. 20 (1), pp. 74–80, January - February 1997.

[16] E. A. Morelli, "Flight-test experiment design for characterizing stability and control of hypersonics vehicles," *Journal of Guidance, Control and Dynamics*, vol. 32 (3), pp. 949–959, May-June 2009.

[17] V. Klein and E. A. Morelli, *"Aircraft System Identification: Theory and Practice"*. Reston, Virginia: AIAA, 2006.